Photodegradation of Substituted Stilbene Compounds: What Colors Aging Paper Yellow?

Bo Durbeej[†,‡] and Leif A. Eriksson*[,§]

Department of Quantum Chemistry, Uppsala University, Box 518, 751 20 Uppsala, Sweden, Department of Cell and Molecular Biology, Uppsala University, Box 596, 751 24 Uppsala, Sweden, and Department of Natural Sciences and Örebro Life Science Center, Örebro University, 701 82 Örebro, Sweden

Received: February 20, 2005; In Final Form: April 29, 2005

Photodegradation of lignin is one of the major postprocessing problems in paper production, as this renders yellowing of the paper and reduced paper quality. In this study, we have explored the photochemical properties of substituted stilbene derivatives believed to be key chromophores in the photodegradation of lignin derived from cinnamyl alcohol. In particular, the present work focuses on the computation of UV/vis electronic absorption spectra for different methoxylated stilbenes and their proposed photodegradation products. All calculations were performed using the time-dependent formalism of density functional theory (TD-DFT) and the B3LYP hybrid functional. It is concluded that the methodology employed is capable of reproducing not only the overall spectra, but also subtle features owing to the effects of different substitution patterns. For the strongly absorbing first excited singlet state (HOMO → LUMO excitation) of the methoxylated stilbenes, the calculated transition energies are, albeit somewhat fortuitously, in excellent agreement with experimental data. The light-induced yellowing indirectly caused by the presence of stilbenes can be rationalized in terms of the absorption spectra of the resulting photodegraded *o*-quinones, for which distinct transitions in the 420−500 nm region of the visible spectrum lacking prior to degradation are observed.

Introduction

A major problem with paper manufactured from pulps produced by mechanical and chemimechanical methods is the tendency of the material to undergo yellowing (brightness reversion) upon exposure to sunlight. There is general agreement that the coloration is due to remaining lignin constituents in the pulp, albeit neither the precise nature of the chromophores responsible for this nor the exact mechanism for their formation has been conclusively established.

One of the most lucid proposals regarding the type of chromophores involved suggests that the yellowing results from the formation of *o*-quinones from diguaiacylstilbenes. These stilbenes are generated during the mechanical grinding, disc refining, and alkaline peroxide treatment of spruce pulps.[1−3] The precursors of the stilbenes, in turn, are diarylpropane units of lignin, i.e., fragments of the amorphous lignin polymer that together with cellulose and hemicellulose makes up the main fraction of the wood fiber cell wall. In the context of this proposal, polyalkylated stilbenes have been shown to be important chromophores,[4,5] and it has been suggested that these compounds undergo photoinduced redox and degradation reactions producing phenoxy-type radicals that in turn react further to form the corresponding *o*-quinones with absorption characteristics yielding a yellow coloration.

Stilbene photodegradation also involves elimination reactions that require the presence of water, whereas the photoconversion of *β*-*O*-4 aryl ether lignin constituents into quinones[6−10] instead requires the presence of molecular oxygen. The latter type of reactions is believed to proceed by way of photoinduced formation of singlet oxygen. For an overview of photoinduced degradation of lignin model compounds, we refer to ref 11.

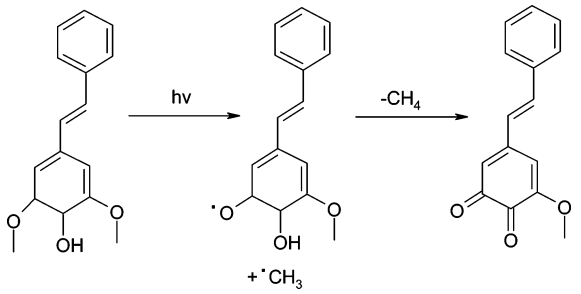

Figure 1. Proposed photochemical degradation of methoxylated stilbenes and subsequent formation of *o*-quinones.

From anaerobic (thus eliminating the possibility of singlet oxygen mediated reactions) photochemical studies of *β*-*O*-4 aryl ether analogues and polyalkoxylated stilbenes, a mechanism underlying the photoinduced yellowing based on the observed formation of low-molecular-weight products methane and ethane has been put forth,[12,13] as outlined in Figure 1.

In the current work, we have chosen to investigate the polymethoxylated stilbenes of ref 13, and their corresponding *o*-quinones, by means of quantum chemical calculations. The aim is to employ the time-dependent density functional theory (TD-DFT)[14,15] formalism to explore the basic photochemical properties of the reactants and products of the photoyellowing mechanism proposed by Weir et al.[12,13] We have previously employed TD-DFT calculations to successfully investigate the properties of a number of naturally occurring chromophores such as astaxanthin[16,17] and phytochromobilin,[18] as well as phototoxic reactions of furocoumarin derivatives[19] and the UV-induced formation and repair of cyclobutane pyrimidine dimers in DNA.[20−22]

* Corresponding author. E-mail: leif.eriksson@nat.oru.se.
† Department of Quantum Chemistry, Uppsala University.
‡ Department of Cell and Molecular Biology, Uppsala University.
§ Örebro University.

10.1021/jp050873l CCC: $30.25
Published on Web 06/04/2005

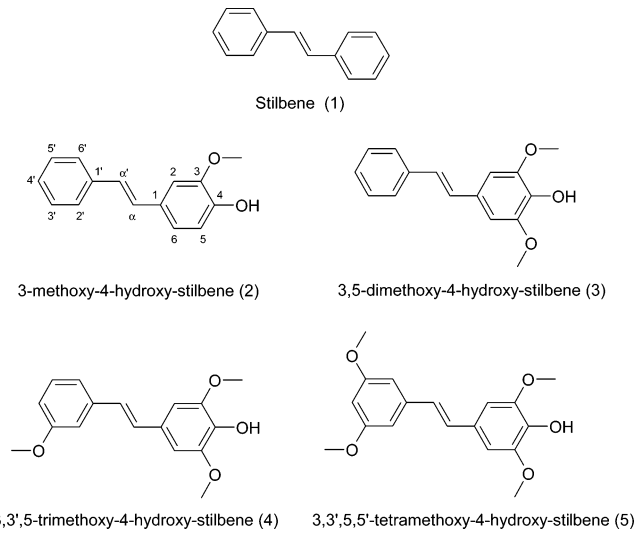

Figure 2. *Trans* stereoisomers of stilbene and substituted stilbene derivatives investigated in the current work.

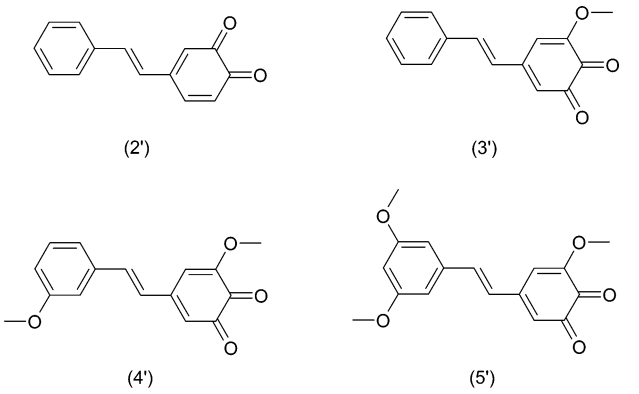

Figure 3. *Trans* stereoisomers of *o*-quinone compounds resulting from photodegradation of the corresponding substituted stilbenes shown in Figure 2.

A number of excited-state quantum chemical investigations of the parent stilbene compound, and derivatives thereof, have previously been reported, albeit primarily focusing on accurate determination of absorption spectra and investigating photochemically induced *cis-trans* isomerizations. In this context, we mention, e.g., the very accurate CASPT2 studies by Molina et al.[23,24] and the recent comparative TD-DFT, CASPT2, and ZINDO/S-CIS study by Kwasniewski et al.[25]

Theoretical Method

The model compounds investigated in the current work are depicted in Figure 2 and range from unsubstituted stilbene (**1**) to 3,3′,5,5′-tetramethoxy-4-hydroxystilbene (**5**) in their *trans* configurations. In addition, the *cis* stereoisomers of **1** and **5** are subjected to calculations as well. The primary focus is on the effects of methoxy substitution and photodegradation of these compounds—yielding *o*-quinones (Figure 3)—on their electronic absorption spectra.

The geometries of all systems were optimized using the B3LYP hybrid density functional[26−28] in conjunction with the 6-31G(d,p) basis set. Based on optimized ground-state geometries, vertical excitation energies were then calculated employing TD-DFT[14,15] at the B3LYP/6-31+G(d,p) level. The inclusion of diffuse functions in the basis set is often a crucial prerequisite for accurate determination of excitation energies,[19] whereas their effect on geometric structures generally is less pronounced when dealing with neutral systems. From thorough quantum chemical calculations on unsubstituted stilbene reported by Deleuze and co-workers,[29] it should however be noted that a quantitatively accurate description of the torsion angles between the phenyl rings and the 2-butene linker in *trans*-stilbene requires a large basis set incorporating also diffuse functions. Furthermore, this study also showed that B3LYP tends to overemphasize the planarity of stilbene.[29] While the present work focuses on the calculation of electronic absorption spectra of stilbene derivatives and their *overall*—rather than *absolute*—dependence on torsional motion, these findings, which from the point of view of the general conclusions to be drawn herein are of less significance, should in the following nevertheless be kept in mind. The previously noted tendency of TD-DFT underestimating excitation energies for high-energy transitions[30] was observed also in the present study.

The effect of rotational motion of a phenyl ring on stilbene light absorption was explored by freezing either of two different dihedral angles in steps of 5° (up to 45°) and by subsequently, after relaxing all other geometric degrees of freedom at each point, performing TD-B3LYP/6-31+G(d,p) single-point calculations.

All calculations were carried out using the Gaussian 98 and Gaussian 03 program packages.[31,32]

Results and Discussion

Geometric Features. In all *trans*-stilbene and *trans-o*-quinone systems, the two benzene rings are found to be coplanar or very nearly coplanar, in line with the findings of Deleuze et al.[29] Some repulsive effects prevail between the ring hydrogens at the C2/C6 positions and the hydrogens of the 2-butene linker, which in a few cases lead to slight out-of-plane rotations of the rings. All such distortions occur about the C1−Cα bonds, whereas the linker fragment in all cases remains entirely planar. In unsubstituted stilbene and in compound **3**, the rings are rotated ca. 5° out-of-plane; in compound **5** the rotations are slightly larger, due to stronger interactions caused by the bulky substituents.

The methoxy groups in the hydroxylated rings display a common rotational pattern relative to the ring plane. In the stilbenes, one methoxy group lies in the plane of the ring, with the methoxy group pointing away from the hydroxy group. The other methoxy carbon is rotated ca. 60° out of the ring plane (dihedral angle C_{Me}−O3−C3−C4). Upon formation of the *o*-quinone, the out-of-plane methoxy group attains a dihedral angle of approximately 25°. Thermal energy can, however, be expected to cause the methoxy groups to either rotate freely or at least perform wagging, semicircular motion in that repulsive effects may hinder full rotation to the other side of the ring plane.

The bond lengths of the linker fragments remain essentially unaltered upon formation of the *o*-quinones and display a clear alternating pattern with single/double/single bond character. The same holds true for the nonhydroxylated rings. The hydroxylated rings, on the other hand, undergo large changes in bond lengths caused by quinone formation. The pattern is very similar for all systems explored; in Figure 4 we show the optimized structures of compound **5** and its *o*-quinone (**5′**). The main effect is a significant elongation of the C4−C5 bond (connecting the two keto groups) from 1.41 to 1.56 Å, and elongation of the C3−C4 bond by close to 0.1 Å. The overall structures of the quinone rings reveal that the bonds attain more distinct single/double bond characters as compared to the benzene-like geometry prior to quinone formation (bond lengths fluctuating between 1.39 and 1.41 Å).

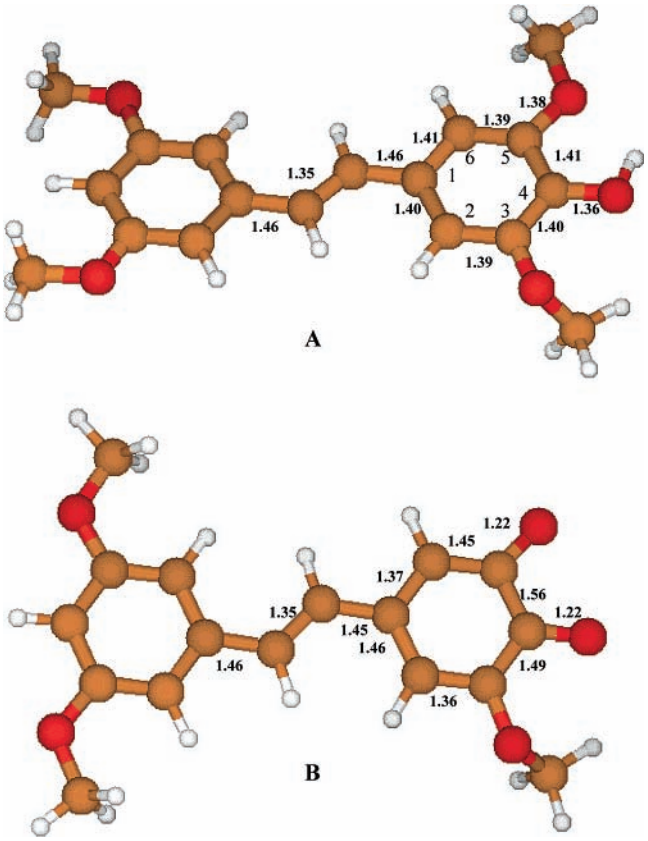

Figure 4. Optimized structures of compounds **5** (A) and **5′** (B).

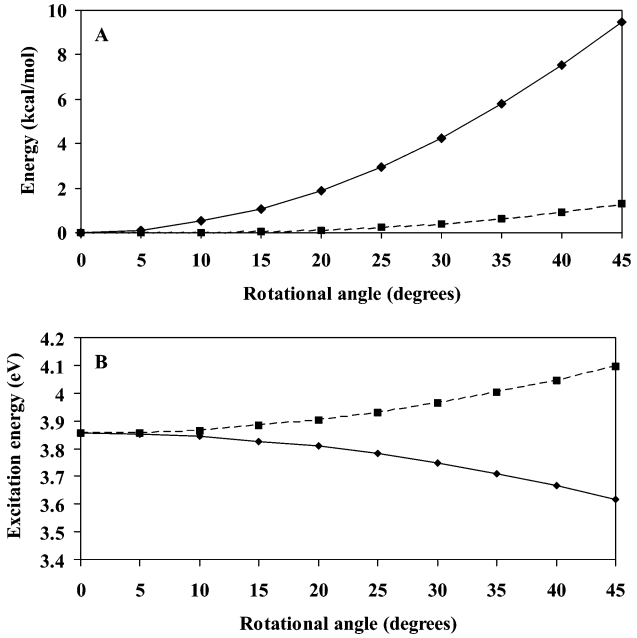

Figure 5. Effects of rotation about the Cα−Cα′ bond (diamonds) and the Cα−C1 bond (squares) in *trans*-stilbene. (A) Relative ground-state energy (kcal/mol); (B) vertical $S_0 \rightarrow S_1$ excitation energy (eV).

In the *cis*-form of stilbene (**5**) and its *o*-quinone derivative, very large out-of-plane distortions are noted due to the repulsive interaction between the bulky phenyl rings. The central C1−Cα−Cα′−C1′ fragment attains a dihedral angle of 6−7°, whereas both rings are rotated by another 32−35° out of the plane (Cα′−Cα−C1−C2 and Cα−Cα′−C1′−C2′ dihedrals). Similar angles are found also in the unsubstituted *cis*-stilbene.

The thermodynamic stability of the photodegradation products may be estimated by comparing the energy of the parent compounds with the sum of the energies of the resulting fragmentation products (quinone and methane). For all systems investigated, the overall reaction outlined in Figure 1 is endothermic. For compound **2**, the endothermicity is the largest, 17.9 kcal/mol. The remaining systems all carry an additional methoxy fragment in the *o*-quinone ring, which appears to reduce the endothermicity somewhat, to 14.8−15.1 kcal/mol. In addition, **5** and **5′** are ca. 5.5 kcal/mol more stable than the corresponding *cis* stereoisomers.

Rotation of Stilbene Rings. To explore the rotational flexibility of the stilbenes, and the effects of vibrational motion on electronic absorption, ground-state B3LYP/6-31G(d,p) geometry optimizations and subsequent TD-B3LYP/6-31+G(d,p) vertical excitation energy calculations were performed for a number of structures representing rotation about the Cα−Cα′ and Cα−C1 bonds in unsubstituted *trans*-stilbene. The results are shown in Figure 5. As expected (Figure 5A), rotation about the Cα−Cα′ bond (the "π-bond", initially $R = 1.35$ Å) is associated with a considerably higher energy cost than rotation about one of the Cα−C1 "single" bonds (initially $R = 1.46$ Å). Upon rotation of either bond up to 45°, only marginal effects are seen on the bond lengths.

For the Cα−Cα′ bond rotation, the overlap between the two p-orbitals of the Cα carbons is broken at approximately 45°, and the associated energy thereby rises dramatically. If we, for example, compare the two systems having a thermal energy of 1 kcal/mol available to induce rotational motion, we note that the motion about the central Cα−Cα′ bond will be less than ±15°, whereas fluctuations above ±40° are allowed around the Cα−C1 bonds. We may thus conclude that the benzene rings will undergo wagging or rotational motions at a low energy cost, whereas the linker moiety is considerably more rigid.

Turning to the effect of vibrational motion on electronic absorption, the calculated spectra—covering the region from 3.86 to 6.13 eV (321 to 202 nm)—are dominated by the $S_0 \rightarrow S_1$ HOMO → LUMO transition ($\Delta E = 3.86$ eV, oscillator strength $f = 0.91$) and the $S_0 \rightarrow S_5$ HOMO − 1 → LUMO transition ($\Delta E = 5.04$ eV, $f = 0.21$). All other transitions are associated with significantly smaller oscillator strengths. In Figure 5B, we display the $S_0 \rightarrow S_1$ excitation energy as a function of the two rotational angles investigated. The two rotations are found to act in different ways regarding the magnitude of the transition energy. For the rotation about the central π-bond, ΔE decreases by 0.24 eV (corresponding to an increase in λ_{max} from 322 to 343 nm) during the 45° rotation. For the wagging motion of the benzene rings, on the other hand, ΔE increases by roughly the same amount (corresponding to a decrease in λ_{max} from 322 to 303 nm) during the 45° motion. At the same time the transition probability is lowered somewhat, from 0.91 to 0.79 and 0.84 for the two rotations, respectively. Given that the wagging motion about the Cα−C1 bonds requires far less energy, it can be concluded that vibrational motion will shift the main absorption in *trans*-stilbene (the HOMO → LUMO excitation) toward slightly shorter wavelengths (i.e., blue-shifted absorption), compared to the value for the static, optimized, structure.

While the above analysis strictly speaking refers to the effect of zero-point vibrational motion on electronic absorption, a more complete analysis would have to explicitly take into account the influence of temperature as well. This can be accomplished by combining classical molecular dynamics (MD) simulations at finite temperature with (zero-temperature) excited-state quantum chemical calculations. For example, MD simulations

TABLE 1: Vertical Singlet Excitation Energies (Upper Row, Energies in eV (nm); Lower Row, Oscillator Strengths) Computed at the TD-B3LYP/6-31+G(d,p) Level for Stilbenes 1−5 (cf. Figure 2)

system	ΔE, eV (nm) f	ΔE, eV (nm) f	ΔE, eV (nm) f	ΔE, eV (nm) f	ΔE, eV (nm) f
1[a]	3.86 (322)	4.48 (277)	5.04 (246)	6.13 (202)	
	0.91	0.03	0.21	0.06	
cis-**1**	3.99 (311)	5.02 (247)	5.49 (226)		
	0.38	0.23	0.11		
2	3.62 (342)	4.39 (282)	4.66 (266)	4.95 (251)	5.78 (214)
	0.87	0.05	0.21	0.13	0.05
3	3.63 (342)[b]	4.38 (283)	4.65 (266)	4.68 (265)	4.84 (256)
	0.87	0.04	0.03	0.08	0.16
4	3.60 (345)[c]	4.62 (268)	4.81 (258)	5.54 (224)	
	0.90	0.11	0.14	0.04	
5	3.61 (343)[d]	3.96 (313)	4.81 (258)	5.10 (243)	5.29 (235)
	0.90	0.04	0.15	0.03	0.15
cis-**5**	3.72 (333)	3.96 (313)	4.83 (266)	4.89 (255)	5.21 (238)
	0.23	0.18	0.08	0.15	0.07

[a] Experimental and other theoretical values: see, e.g., ref 25. [b] Experimental value: 340 nm.[13] [c] Experimental value: 342 nm.[13] [d] Experimental value: 350 nm.[13]

of oligomer chains of poly(*p*-phenylene vinylene) using the MM3 force field in conjunction with computationally inexpensive ZINDO/S-CIS calculations have shown that thermal motion at room temperature may result in broadening of the first absorption band (λ_{max}) at half the maximum by up to 23 (*trans*-stilbene) and 33 nm (*cis*-stilbene), respectively.[33] Furthermore, λ_{max} becomes blue-shifted due to temperature effects,[33] which the present calculations also suggest.

Excitation Spectra of Substituted Stilbenes and their *o*-Quinones. In the experimental study by Weir et al.,[13] UV/vis absorption and emission spectra were recorded for the methoxylated stilbenes (**3**−**5**) of Figure 2, as a function of time during up to 5 min irradiation at $\lambda \geq 300$ nm. It was concluded that the absorption maxima of the nondegraded stilbenes lie at 340, 342, and 350 nm, respectively, with the corresponding extinction coefficients equal to 4×10^4, 3.1×10^4, and 3.4×10^4 dm^3 mol^{-1} cm^{-1}. After only a few seconds, a significant reduction of absorption in the 340−350 nm wavelength region was noted, concomitant with a buildup of absorption at wavelengths above 400 nm and in the 300−320 nm region. This was accompanied by a simultaneous yellow coloration of the samples.

The vertical singlet excitation energies for the more probable transitions ($f \geq 0.03$) in substituted *trans*-stilbenes (**2**−**5**), computed at the present TD-B3LYP/6-31+G(d,p) level of theory, are listed in Table 1. Many of the 15 transitions computed were found to have near-zero oscillator strength and hence are irrelevant from the point of view of coloration. We note that the dominating transition, which occurs at around 340 nm with oscillator strength ∼0.9 and corresponds to a HOMO → LUMO transition to the first excited singlet state, is predicted in excellent agreement with experimental data.

Generally, TD-DFT employing standard exchange-correlation functionals (such as B3LYP) enables accurate calculations of low-lying valence excited states of unsaturated organic compounds,[34−37] but fails to account for excitations to Rydberg states.[36,38] Furthermore, TD-DFT typically yields considerable errors for transitions involving extensive charge transfer.[36,37,39−41] The accuracy of TD-DFT excitation energies is largely dependent on the quality of both occupied and virtual Kohn−Sham orbitals and eigenvalues, and the failure of TD-DFT to treat Rydberg states is related to the fact that the incorrect asymptotic behavior of the exchange-correlation potential of conventional functionals leads to a poor description of virtual orbitals.[38] The erroneous treatment of charge-transfer excited states, in turn, seems to be due to the self-interaction error in the orbital energies from the ground-state calculation that precedes the actual linear response TD-DFT calculation from which the excitation energies are obtained.[41] Even though the above shortcomings are of minor importance for the first excited singlet state of stilbenes, it is nevertheless obvious that the excellent agreement with experimental data should be regarded as somewhat fortuitous.

The next set of strong transitions ($f \geq 0.1$) occurs at considerably shorter wavelengths: in the 240−270 nm range, or ca. 1 eV above the HOMO → LUMO transition. For the *cis* form of stilbene (**5**), the conjugation over the full system is reduced due to the noncoplanarity of the phenyl rings. Hence, the lowest energy transition occurs at a shorter wavelength (333 nm) and is associated with a significantly smaller oscillator strength ($f = 0.23$) than the corresponding transition in *trans*-**5** (343 nm, $f = 0.90$). In addition, the absorption characteristics of *cis*-**5** differ from that of *trans*-**5** by exhibiting an additional, strong transition at 313 nm. These two transitions, at 333 and 313 nm, in some sense agree with the observations of Weir et al.,[13] of the occurrence of UV absorption around 320 nm in the spectra of **4** and **5**, which they attributed to UV-induced isomerization to the corresponding *cis* configurations.

The low-lying singlet excitations with appreciable oscillator strength in the *o*-quinones are listed in Table 2. The electronic spectra for these systems are markedly different from those of the nondegraded stilbenes by exhibiting strong absorption in the 2.5−2.9 eV (496−428 nm) region. According to the calculations, *o*-quinone (**2′**) will absorb blue-green light, and thus display an orange-red coloration. For **3′** and *cis*-**5′**, the main absorption takes place in the blue-violet borderline region, corresponding to yellow/orange coloration. Compounds **4′** and **5′**, finally, absorb in the middle of the blue region of the spectrum, and display orange coloration. However, as there are several transitions in these wavelength regimes, the exact color of the samples is difficult to specify.

It should be noted that the lowest lying singlet excitation for all *o*-quinone systems (not included in Table 2) occurs at around 650 nm (1.8−1.9 eV), albeit with oscillator strength very close to zero. Compounds **3′**−**5′** also exhibit a low-lying HOMO → LUMO excitation in the 560−580 nm (2.1−2.2 eV) range. The complementary color for the latter transition is in the blue/violet spectral region. However, this transition occurs with oscillator strength well below 0.1, and is thus less likely to account for the displayed coloration.

TABLE 2: Vertical Singlet Excitation Energies (Upper Row, Energies in eV (nm); Lower Row, Oscillator Strengths) Computed at the TD-B3LYP/6-31+G(d,p) Level for *o*-Quinones 2′−5′ (cf. Figure 3)

system	Δ*E*, eV (nm) *f*	Δ*E*, eV (nm) *f*	Δ*E*, eV (nm) *f*	Δ*E*, eV (nm) *f*	Δ*E*, eV (nm) *f*	Δ*E*, eV (nm) *f*
2′	2.52 (492)	3.40 (365)	3.44 (361)	4.15 (299)	4.61 (269)	5.33 (233)
	0.22	0.13	0.05	0.70	0.13	0.13
3′	2.19 (567)	2.83 (438)	3.91 (317)	4.19 (296)	4.34 (286)	4.58 (271)
	0.06	0.35	0.50	0.05	0.16	0.08
4′	2.16 (573)	2.56 (478)	2.96 (419)	3.88 (320)	4.10 (303)	4.59 (270)
	0.07	0.17	0.17	0.48	0.19	0.11
5′	2.16 (574)	2.61 (476)	3.94 (315)	4.08 (304)	5.17 (240)	
	0.08	0.28	0.71	0.07	0.13	
cis-**5′**	2.80 (442)	3.71 (334)	4.17 (297)	4.69 (265)	4.81 (258)	5.20 (238)
	0.15	0.07	0.17	0.05	0.05	0.11

According to Weir et al.,[13] compounds **4** and **5** displayed significant UV absorption at 320 nm upon irradiation, concomitant with the coloration of the samples. As noted above, one explanation for this observation could be the formation, through photoinduced isomerization, of the corresponding (nondegraded) *cis*-stilbenes. However, as seen from Table 2, the three (degraded) *trans*-*o*-quinones **3′**, **4′**, and **5′** all exhibit maximum absorption between 315 and 320 nm. Given also the more pronounced absorption of these compounds in the visible spectrum (in contrast to *cis*-**5**), it is more likely that the observed spectral changes are caused by degrading stilbenes (i.e., the *o*-quinones) than by *cis*-*trans* isomerization of the parent stilbenes.

Summary

We have in the current work explored the structures and UV/vis absorption spectra of a series of methoxylated stilbenes and their *o*-quinone photodegradation products using the B3LYP hybrid density functional and TD-DFT for the calculation of vertical excitation energies. For unsubstituted *trans*-stilbene, the results are in good agreement with previous theoretical data and experiments (cf. ref 25 and references therein). Asymmetric methoxylation/hydroxylation of the compounds is found to lower the $S_0 \rightarrow S_1$ excitation by ca. 0.20−0.25 eV and introduce a splitting of the second lowest strong transition.

The main absorption at 340−350 nm observed experimentally for the three methoxylated stilbenes **3**−**5**[13] is reproduced at the current level of theory, and the yellow/orange coloration of the samples and the appearance of UV absorption at ca. 320 nm are rationalized in terms of photodegradation-mediated formation of *o*-quinones **3′**, **4′**, **5′**.

The effect of torsional motion around the 2-butene linker on ground-state energy and $S_0 \rightarrow S_1$ excitation energy was explored for the unsubstituted *trans*-stilbene system, and it was concluded that the benzene rings will be able to undergo relatively free wagging motion resulting in an increase in excitation energy by 0.1−0.2 eV, whereas the linker fragment is highly rigid.

Subsequent work, currently under way, involves detailed exploration of mechanistic features of photodegradation mechanisms, as well as calculation of absorption spectra of *β*-*O*-4 aryl ethers and their degradation products.

Acknowledgment. This work was funded by the Swedish Science Research Council (VR) and the Wood Ultrastructure Research Center (WURC). Grants of computing time at the National Supercomputing Center (NSC) in Linköping are also gratefully acknowledged.

Supporting Information Available: This material is available free of charge via the Internet at http://pubs.acs.org.

References and Notes

(1) Zhang, L.; Gellerstedt, G. *Acta Chem. Scand.* **1994**, *48*, 490−497.
(2) Leigh, W. J.; Lewis, J.; Lin, V.; Postigo, J. A. *Can. J. Chem.* **1996**, *74*, 263−275.
(3) Ruffin, B.; Castellan, A.; Grelier, S.; Nourmamode, A.; Riela, S.; Trichet, V. *J. Appl. Polym. Sci.* **1998**, *69*, 2517−2531.
(4) Gellerstedt, G.; Zhang, L. *J. Wood Chem. Technol.* **1992**, *12*, 387−412.
(5) Wu, Z. H.; Matsouka, M.; Lee, D. Y.; Sumimoto, M. *Mokuzai Gakkaishi* **1991**, *37*, 164−171.
(6) Lebo, S. E.; Lonsky, W. F. W.; McDonough, T. J.; Medvecz, P. J.; Dimmel, D. R. *J. Pulp Pap. Sci.* **1990**, *16*, J139−J143.
(7) Scaiano, J. C.; Netto-Ferreira, J. C.; Wintgens, V. *J. Photochem. Photobiol. A: Chem.* **1991**, *59*, 265−268.
(8) Zhao, B.-J.; Depew, M. C.; Weir, N. A.; Wan, J. K. S. *Res. Chem. Intermed.* **1993**, *19*, 449−462.
(9) Bonini, C.; D'Auria, M.; D'Alessio, L.; Mauriello, G.; Tofani, D.; Viggiano, D.; Zimbardi, F. *J. Photochem. Photobiol. A: Chem.* **1998**, *113*, 119−124.
(10) Müller, U.; Rätzsch, M.; Schwanninger, M.; Steiner, M.; Zöbl, H. *J. Photochem. Photobiol. B: Biol.* **2003**, *69*, 97−105.
(11) Lanzalunga, O.; Bietti, M. *J. Photochem. Photobiol. B: Biol.* **2000**, *56*, 85−108.
(12) Weir, N. A.; Arct, J.; Ceccarelli, A. *Polym. Degrad. Stab.* **1991**, *43*, 409−414.
(13) Weir, N. A.; Arct, J.; Ceccarelli, A. *Polym. Degrad. Stab.* **1995**, *47*, 289−297.
(14) Casida, M. E. In *Recent Advances in Density Functional Methods, Part I*; Chong, D. P., Ed.; World Scientific: Singapore, 1995; pp 155−193.
(15) Stratmann, R. E.; Scuseria, G. E.; Frisch, M. J. *J. Chem. Phys.* **1998**, *109*, 8218−8224.
(16) Durbeej, B.; Eriksson, L. A. *Chem. Phys. Lett.* **2003**, *375*, 30−38.
(17) Durbeej, B.; Eriksson, L. A. *Phys. Chem. Chem. Phys.* **2004**, *6*, 4190−4198.
(18) Durbeej, B.; Borg, O. A.; Eriksson, L. A. *Phys. Chem. Chem. Phys.* **2004**, *6*, 5066−5073.
(19) Llano, J.; Raber, J.; Eriksson, L. A. *J. Photochem. Photobiol. A: Chem.* **2003**, *154*, 235−243.
(20) Durbeej, B.; Eriksson, L. A. *J. Photochem. Photobiol. A: Chem.* **2002**, *152*, 95−101.
(21) Durbeej, B.; Eriksson, L. A. *Photochem. Photobiol.* **2003**, *78*, 159−167.
(22) Durbeej, B.; Eriksson, L. A. *J. Am. Chem. Soc.* **2000**, *122*, 10126−10132.
(23) Molina, V.; Merchán, M.; Roos, B. O. *J. Phys. Chem. A* **1997**, *101*, 3478−3487.
(24) Molina, V.; Merchán, M.; Roos, B. O. *Spectrochim. Acta, Part A* **1999**, *55*, 433−446.
(25) Kwasniewski, S. P.; Deleuze, M. S.; Francois, J. P. *Int. J. Quantum Chem.* **2000**, *80*, 672−680.
(26) Becke, A. D. *J. Chem. Phys.* **1993**, *98*, 5648−5652.
(27) Lee, C.; Yang, W.; Parr, R. G. *Phys. Rev. B* **1988**, *B37*, 785−789.
(28) Stephens, P. J.; Devlin, F. J.; Chabalowski, C. F.; Frisch, M. J. *J. Phys. Chem.* **1994**, *98*, 11623−11627.
(29) Kwasniewski, S. P.; Claes, L.; François, J.-P.; Deleuze, M. S. *J. Chem. Phys.* **2003**, *118*, 7823−7836.
(30) Casida, M. E.; Jamorski, C.; Casida, K. C.; Salahub, D. R. *J. Chem. Phys.* **1998**, *108*, 4439−4449.
(31) Frisch, M. J.; et al. *Gaussian 98*, rev. A.11; Gaussian Inc.: Pittsburgh, PA, 2002.
(32) Frisch, M. J.; et al. *Gaussian 03*, rev. B.03; Gaussian Inc.: Pittsburgh, PA, 2003.

(33) Kwasniewski, S. P.; François, J.-P.; Deleuze, M. S. *J. Phys. Chem. A* **2003**, *107*, 5168−5180.
(34) Bauernschmitt, R.; Ahlrichs, R. *Chem. Phys. Lett.* **1996**, *256*, 454−464.
(35) van Gisbergen, S. J. A.; Rosa, A.; Ricciardi, G.; Baerends, E. J. *J. Chem. Phys.* **1999**, *111*, 2499−2506.
(36) Tozer, D. J.; Amos, R. D.; Handy, N. C.; Roos, B. O.; Serrano-Andrés, L. *Mol. Phys.* **1999**, *97*, 859−868.
(37) Fabian, J. *Theor. Chem. Acc.* **2001**, *106*, 199−217.
(38) Tozer, D. J.; Handy, N. C. *J. Chem. Phys.* **1998**, *109*, 10180−10189.
(39) Dreuw, A.; Weisman, J. L.; Head-Gordon, M. *J. Chem. Phys.* **2003**, *119*, 2943−2946.
(40) Deleuze, M. S. *J. Phys. Chem. A* **2004**, *108*, 9244−9259.
(41) Dreuw, A.; Head-Gordon, M. *J. Am. Chem. Soc.* **2004**, *126*, 4007−4016.